Human group V secretory phospholipase A$_2$ is associated with lipid rafts and internalized in a flotillin-dependent pathway

HAE JIN RHEE[1,2], LITING JI[2], SEUNG-HYUK KIM[3] and JONGHO LEE[3]

[1]Institute of Natural Medicine, [2]Department of Natural Medicine and [3]Department of Pharmacology,
College of Medicine, Hallym University, Chunchon, Kangwon-do 200-702, Republic of Korea

Abstract. The mechanisms of secretory phospholipase A$_2$ (sPLA2) action are not understood clearly. Previously, it was suggested that sPLA2s are internalized into cells for the targeting of sPLA2 to intracellular action sites. However, the mechanisms for sPLA2 internalization remain to be identified. The present study demonstrated for the first time that human group V sPLA2 (hVPLA2) is associated with lipid rafts and is internalized in a flotillin-dependent pathway. The lipid raft association was probed by cholesterol-sensitive enrichment of hVPLA2 in low-density fractions and co-patching of ganglioside GM1 rafts through cross-linking of hVPLA2 in HEK293 and CHO cells. The hVPLA2 associated with lipid rafts was shown to be internalized into HEK293 cells at a relatively rapid rate ($t_{1/2}$ =16 min) and this internalization was inhibited by the knockdown of flotillin-1, but not by chlorpromazine, an inhibitor of clathrin-mediated endocytosis. Moreover, internalized hVPLA2 was shown to be colocalized extensively with flotillin-1 in a punctate structure, but not caveolin-1. These data revealed that the internalization of hVPLA2 is mediated by flotillin-1. Attenuation of arachidonic acid release from plasma membrane through the association of hVPLA2 with lipid rafts suggested that this association with lipid rafts may be important in protecting mammalian cells from excessive degradation of plasma membrane and trafficking hVPLA2 into intracellular targets.

Introduction

Phospholipase A$_2$ (PLA2) catalyzes the hydrolysis of membrane phospholipids, the products of which can be transformed into potent inflammatory lipid mediators, platelet-activating factor and eicosanoids, which include prostaglandins, thromboxanes, leukotrienes and lipoxins. Multiple forms of PLA2s have been identified in mammalian tissues, including 10 secretory PLA2s (sPLA2s; group IB, IIA, IIC, IID, IIE, IIF, III, V, X and XIIA), six Ca^{2+}-dependent PLA2s (group IV) and six Ca^{2+}-independent PLA2s (groups VI) (1,2).

Group IV cytosolic PLA2 (cPLA2)-α is known to release arachidonic acid (AA) from phospholipids as the first step for the biosynthesis of eicosanoids. Increasing data suggest that sPLA2 can play a role in eicosanoid production. Expression of group IIA sPLA2 (IIAPLA2) in HEK293 or mouse mesangial cells induces AA in a cPLA2-α-dependent manner (3,4). Previous studies showed that the addition of IIAPLA2 or VPLA2 to mammalian cells leads to the generation of eicosanoids in a cPLA2-dependent or -independent manner (5-7). Since sPLA2 is a secretory enzyme and accumulated in inflammatory exudates, it has been proposed that sPLA2 is secreted to extracellular medium upon stimulation and acts on target cells. However, IIAPLA2 may be scarcely able to release AA from plasma membrane without internalization or priming by proinflammatory cytokines, because IIAPLA2 as a highly basic protein revealed poor interfacial binding to phosphatidylcholine (PC), a major phospholipid on the outer leaflet of the plasma membrane in mammalian cells. Consistent with this speculation, previous studies have demonstrated that IIAPLA2 was internalized and promoted AA release and prostaglandin E$_2$ production in rat fibroblast or stable HEK cells expressing mouse IIAPLA2 when the cells were treated with inflammatory cytokines (8,9). Moreover, sPLA2, including IIAPLA2, human group V sPLA2 (hVPLA2) and gXPLA2 can act transcellularly to a different extent to generate AA in distal cells via the paracrine mechanism (10-12). Thus, endocytosis and trafficking of sPLA2 plays an essential regulatory role in the physiological function of sPLA2, including inflammation and atherosclerosis. However, the mechanisms by which sPLA2 is internalized in mammalian cells and the spatio-temperal mobilization of internalized sPLA2 is regulated are poorly understood, although basic sPLA2s such as IIAPLA2 and hVPLA2 are shown to bind to heparan sulfate proteoglycan (HSPG) and to be colocalized with caveolin (4,13).

In the present study, we investigated the molecular mechanism for the internalization of hVPLA2 in CHO and HEK293 cells. To the best of our knowledge, in the present study, we

Correspondence to: Professor Hae Jin Rhee, Institute of Natural Medicine, Hallym University, Hallymdaehak-gil, Chunchon, Kangwon-do 200-702, Republic of Korea
E-mail: hjrhee@hallym.ac.kr

Professor Jongho Lee, Department of Pharmacology, College of Medicine, Hallym University, Hallymdaehak-gil, Chunchon, Kangwon-do 200-702, Republic of Korea
E-mail: jongholee@hallym.ac.kr

showed for the first time that hVPLA2 is associated with lipid rafts partly by binding to heparan sulfate and internalized in a flotillin-dependent pathway. Flotillin-mediated endocytosis led to trafficking of some hVPLA2 to non-lysosomal vesicles in addition to lysosomal compartments and then to Golgi apparatus. Moreover, the association of hVPLA2 with lipid rafts caused the attenuation of AA release from plasma membrane. These data therefore suggested that the association of hVPLA2 with lipid rafts may be important in protecting the plasma membrane from excessive degradation and increasing AA release and eicosanoid production coupled with the AA release from intracellular targets.

Materials and methods

Materials. Antibodies against syndecan-1, syndecan-4, caveolin-1 and FITC-conjugated antibody against GM130 were purchased from BD Transduction Laboratories (San Diego, CA, USA). Antibodies specific for flotillin-1 and human lysosomal-associated membrane protein (Lamp)-2 were purchased from Santa Cruz Biotechnology, Inc. (Santa Cruz, CA, USA). Antibodies recognizing rat Lamp-2 were purchased from Zymed Laboratories (South San Francisco, CA, USA). Monoclonal antibody specific to hVPLA2 was prepared as described previously (6). Methy-β-cyclodextrin (MβCD), filipin III, fumonitin B1, chlorpromazine HCl, brefeldin A and all other reagents were of an analytical grade and were obtained from Sigma-Aldrich (St. Louis, MO, USA). Dulbecco's modified Eagle's medium (DMEM), Ham, Hank's balanced salt solution (HBSS) and fetal bovine serum (FBS) were from Life Technologies (Carlsbad, CA, USA). HEK293, human embryonic kidney cells and CHO-K1, Chinese hamster ovary cells were purchased from the American Type Culture Collection (Manassas, VA, USA). Fatty acid-free bovine serum albumin (BSA) was purchased from Bayer, Inc. (Kankakee, IL, USA). Recombinant hVPLA2 and its mutants were expressed and purified to homogeneity, as described in a previous study (14). We used recombinant hVPLA2-W79A instead of wild-type and designated hVPLA2-W79A as hVPLA2 throughout the present study, since wild-type purification of W79A-hVPLA2 was much easier than that of wild-type and hVPLA2-W79A was demonstrated to be essentially the same as wild-type hVPLA2 (15).

Cell culture. CHO and HEK293 cells were grown in Ham and DMEM, respectively, supplemented with 10% FBS, 100 U/ml penicillin G and 100 μg/ml streptomycin sulfate in a humidified atmosphere of 95% air and 5% CO_2 at 37˚C. Cell viability after chemical treatment was determined by 0.4% trypan blue staining.

Determining internalization rates. HEK293 cells were plated in a 60-mm dish and cultivated until cells reached subconfluence. The cells were washed with HBSS and incubated in Krebs-HEPES buffer (KHB; 140 mM NaCl, 4 mM KCl, 1 mM $CaCl_2$, 1 mM Na_2HPO_4, 1 mM $MgCl_2$, 10 mM HEPES, pH 7.4, 11.7 mM glucose, 0.2% BSA) containing 150 nM hVPLA2 for 10 min at 4˚C and transferred to 37˚C. Incubation was quenched by the addition of ice-cold PBS at appropriate times. PLA2 bound to the surface was recovered by washing with PBS containing 0.8 M NaCl. Cells were lysed by incubation with lysis buffer (20 mM Tris-HCl, 50 mM NaCl, 1 mM EDTA, pH 7.4) containing 0.4% Nonidet P-40, 1 mM NaF, protease inhibitor mix 20 min on ice. After brief sonication, the cell lysates were centrifuged at 10,000 x g for 3 min. Activities of PLA2 bound to the surface, internalized and remained in medium were assayed, respectively, by measuring the initial rate of [^{14}C]SAPC (Amersham Biosciences Ltd., Little Chalfont, Buckinghamshire, UK) hydrolysis as described previously (14). The rate of internalization was determined by fitting the data to a single-phase exponential curve.

siRNA knockdown. The following RNA duplexes with overhanging dTs for human flotillin-1 and scrambled, non-specific control were prepared from IDT as described previously (16): human flotillin-1 (sense), 5'-UGAGGCCAUGGUGGUCUCC dTdT-3', scrambled control, 5'-UAGCUCGUGGGGCAGUCC dTdT-3'. To assess the effect of siRNA on the endocytosis of hVPLA2, HEK293 cells were transfected with 200 nM of the RNA duplex using Oligofectamine (Invitrogen, Carlsbad, CA, USA) as per the manufacturer's instructions. Two days after transfection, 150 nM hVPLA2 was added to the cells. The cells were incubated at 4˚C for 10 min and 37˚C for 30 min, and the amount of internalized hVPLA2 was determined as described earlier.

AA release assay. Cells were plated onto 35-mm dish and cultivated for two days. Radiolabeling of HEK293 or CHO cells was achieved by incubating the cells with 0.5 μCi/ml [^{3}H] AA (American Radiolabeled Chemicals, St. Louis, MO, USA.) for 12 h at 37˚C. MβCD was treated for 90 min. After washing the cells twice with DMEM containing 0.2% BSA, followed by washing with DMEM, the cells were treated with 150 nM prediluted hVPLA2 in the medium at the specified times. After quenching of the reaction by adding 2 ml of ice-cold DMEM, the cells were separated immediately by centrifugation. The radioactivity of the pellet and supernatant, respectively, was measured by liquid scintillation counter.

Detergent solubilization and OptiPrep gradient fractionation. The HEK293 or CHO cells were plated in 100-mm dishes and cultivated in a monolayer for 2 days. The cells were treated with 100 nM wild-type hVPLA2, hVPLA2-W79A, or hVPLA2-W79A/R100E/K101E for 30 min at 10˚C and washed twice in ice-cold HBSS and once in ice-cold hypotonic solution (42 mM KCl, 5 mM $MgCl_2$, 10 mM HEPES, pH 6.5). The cells were incubated in the hypotonic solution, supplemented with a Protease Inhibitor Mix (Roche Diagnostics, Indianapolis, IN, USA) for 15 min on ice and lysed by passing through 25-gauge needle. Following the addition of sucrose to make a final 0.25 M, cell lysates were sonicated briefly. The lysates were centrifuged at 300 x g for 10 min at 4˚C and resulting supernatants were centrifuged at 10,000 x g for 10 min at 4˚C. The membrane pellets were resuspended in 0.6 ml of 0.5% Triton X-100 or 1% Brij-58 (Pierce Chemical Co., Rockford, IL, USA) in 20 mM NaCl/5 mM EDTA 50 mM Tris, pH 7.4 (TSE) containing a protease inhibitor mix and 0.25 M sucrose and incubated for 30 min at 4˚C. The solublilized lysates were mixed with 1.2 ml of cold 60% OptiPrep (Life Technologies) for 10 min and overlaid successively with 2 ml of 35, 30, 25, 20

and 0% OptiPrep in TSE. After centrifugation at 52,000 x g in a Sorvall TH-641 rotor (Thermo Scientific, Asheville, NC, USA) for 1.5 h at 4°C, six fractions were collected from the top of the gradient. The fractions were TCA precipitated and analyzed by western blot analysis.

Internalization of hVPLA2 and western blot analysis. HEK293 and CHO cells were treated with 100 nM of hVPLA2 or hVPLA2-W79A/R100E/K101E for the indicated period and the incubation was quenched by adding a solution of ice-cold 0.8 M NaCl in DMEM or Ham. After washing with the same solution, the pellet was collected by scraping and centrifugation, then lysed in 100 μl of lysis buffer (20 mM Tris-HCl, 50 mM NaCl, 5 mM EDTA, pH 7.4) containing 0.5% Nonidet P-40, 1 mM NaF, protease inhibitor mix and 0.1% deoxycholic acid. After incubation for 20 min on ice, the cell lysates were sonicated briefly and centrifuged at 12,000 x g for 2 min. The supernatants were analyzed for protein concentration by BCA (Pierce Chemical Co.). Equal amounts of the samples were subjected to 16% sodium dodecyl sulfate-polyacrylamide gel electrophoresis (SDS-PAGE). The electrotransfer of proteins from the gels to polyvinylidene fluoride (PVDF) membrane was achieved using a semidry system (400 mA, 120 min). The membrane was blocked with 2% BSA for 60 min, then incubated with 1 μg/ml of the anti-hVPLA2 monoclonal antibody 3G1 diluted in Tris-buffered saline plus 0.05% Tween-20 (TBST) overnight. The membranes were washed three times for 20 min with TBST. Goat anti-mouse IgG conjugated with horseradish peroxidase was diluted 3,000-fold in TBST and incubated with the PVDF membrane for 60 min. The membrane was washed three times with TBST and analyzed with an ECL chemiluminescence system (Amersham Biosciences).

Antibody-induced patching, immunofluorescence and confocal microscopy. For the patching experiments, CHO cells were plated on cover glass and incubated at 37°C with 5% CO$_2$ for two days. The cells were incubated with hVPLA2 (150 nM) diluted in culture media containing 20 mM HEPES for 20 min at 12°C. After washing with cold HBSS three times, the cells were incubated with mouse anti-hVPLA2 (5 μg/ml) diluted in HBSS containing 2% BSA for 30 min at 12°C. For the clustering of syndecan, the cells were treated with rat anti-syndecan-4 (1/25) or anti-syndecan-1 (1/25) for 10 min at 12°C, which was dialyzed against PBS and diluted in the Ham containing 20 mM HEPES. For further patching, the cells were incubated with Alexa568-conjugated anti-mouse IgG (1/100) or Alexa488-conjugated anti-rat IgG (1/100) diluted in HBSS containing 2% BSA for 30 min at 12°C. Control cells were treated with HBSS-2% BSA and non-immune serum. After washing with HBSS six times, the cells were fixed with 4% formaldehyde for 4 min followed by fixing in -20°C methanol for 1 min. After washing with PBS three times, copatching of GM1 was revealed by incubation of Alexa488-cholera toxin B subunit (Alexa488-CT, 15 μg/ml; Life Technologies) or Alexa568-CT (15 μg/ml) for 30 min under gentle rocking. After washing five times with PBS, the slide was mounted with Fluoromount-G (Southern Biotech Associates, Birmingham, AL, USA). For immunofluorescence experiments, the cells were plated onto a sterile cover glass. The cells were treated with 100 nM of hVPLA2 in culture

media at a 37°C in a 5% CO$_2$ humidified incubator. At the specific time-point, the cells were washed twice with cold PBS and were then fixed at room temperature with 3.6% paraformaldehyde in PBS for 10 min. After fixation, the cells were washed three times with PBS and placed in a blocking solution (10% normal goat serum and 100 μM goat IgG in PBS) at room temperature for 1 h. The cells were then permeabilized with PBS containing 0.1% Triton X-100 and 2% BSA for 1 h at room temperature, washed four times with PBS and incubated with the monoclonal antibodies raised against hVPLA2 and rabbit anti-human caveolin-1 or goat anti-human flotillin-1 (Santa Cruz Biotechnology, Inc.) or rabbit anti-rat Lamp-2, respectively, in the presence of 2% BSA. After overnight incubation at 4°C or 1 h at room temperature, the antibodies were removed and the cells were washed six times with PBS. A secondary antibody, Alexa488 donkey anti-goat antibody or Alexa488 donkey anti-rabbit antibody (both from Molecular Probes) diluted in PBS containing 2% BSA, was applied for 1 h at room temperature followed by washing and incubation with another secondary antibody, Alexa568 donkey anti-mouse antibody (Molecular Probes) diluted in PBS containing 2% BSA for 1 h at room temperature. Golgi apparatus was stained by incubation with FITC-conjugated anti-GM130 for 1 h. After washing six times with PBS, the slide was mounted with Fluoromount-G (Southern Biotech Associates). Imaging was performed using a LSM 5 PASCAL confocal microscope.

Statistical analysis. Results are expressed as mean ± SEM. Statistical significances were analyzed by one-way ANOVA followed by paired t-test using Prism (GradPad Software, La Jolla, CA, USA). P<0.05 was considered statistically significant.

Results

Association of hVPLA2 with detergent-resistant membranes (DRMs). Two different methods can be applied for studies on the cellular trafficking or action mechanism of PLA2. One method involves monitoring endogenous protein by indirect immuno-histochemistry or by the heterologous expression of the protein fused with fluorescent protein. The other method is based on the detection of proteins added exogenously. Limitations of the first method on the internalization mechanism of sPLA2 include: i) detection of the specific isoform of PLA2 is not feasible due to lack of availability of isoform-specific antibodies; ii) secreted PLA2 level is usually beyond the detection limit of conventional visualization. Even if detection of re-internalized PLA2 is allowed or even if it is visualized by expression of the protein as a fluorescent fusion protein, it is difficult to obtain clear data due to strong interference from the high level of the PLA2 stored endogenously. Therefore, in the present study, we studied the internalization mechanism by use of the exogenous addition of purified hVPLA2 to the cells that express endogenous sPLA2 in very low levels and detected hVPLA2 by a specific monoclonal antibody against hVPLA2 as described previously (14). To address the manner in which hVPLA2 is internalized, we determined first the internalization kinetics in HEK293 cells by quantification of internalized hVPLA2 based on its activity. The half-life of internalization was ~16 min and the plateau level was attained in 70 min (Fig. 1), suggesting that internalization may occur in a clathrin-independent manner,
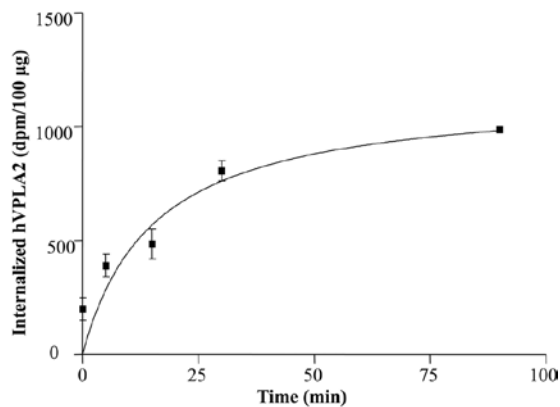
Figure 1. Internalization kinetics of human group V secretory phospholipase A$_2$ (hVPLA2) in HEK293 cells. HEK293 cells were washed with Krebs-Hepes buffer and treated with 150 nM hVPLA2. Internalization of hVPLA2 was quenched in a given interval and quantification of hVPLA2 internalized inside the cells was determined by measuring enzymatic activities of the hVPLA2 using [^{14}C]SAPC as described in Materials and methods. The data present the mean ± SE from three independent experiments run in triplicate.

as clathrin-coated pitch-mediated endocytosis was known to occur within a few minutes. Determination of internalization kinetics using wild-type hVPLA2 showed the essentially same result as that of hVPLA2 (unpublished data). Insolubility to Triton X-100 extraction is a practical criterion for the detection of lipid rafts association with protein. To determine whether hVPLA2 is associated with lipid rafts when hVPLA2 is bound to plasma membrane or internalized, hVPLA2-treated CHO and HEK293 cell lysates were solubilized in 0.5% Triton X-100 and floated onto OptiPrep density gradient. In CHO cells, hVPLA2 was enriched in the low-density membrane fractions containing well-known lipid raft marker, 22-kDa caveolin-1 (Fig. 2A). As the expression levels of caveolin-1 are reported to be low in HEK293 cells, we used 48-kDa flotillin-1 as a lipid raft marker in HEK293 cells. Distribution of flotillin-1 in HEK293 cells showed essentially the same pattern as that of CHO cells (Fig. 2B). When Brij-58 was used to solubilize membrane proteins, both hVPLA2 and flotillin-1 were predominantly partitioned into low-density fractions, whereas hVPLA2 was partitioned more broadly (Fig. 2C). To determine whether hVPLA2-enriched fractions were DRMs, HEK293 cells were treated with MβCD for the depletion of cholesterol and DRMs were isolated from the cell lysates. Most of the hVPLA2 was solubilized by Brij-58 and detected in non-raft fractions along with partial redistribution of flotillin-1 to the non-raft fractions (Fig. 2D, lane 4-6). These data showed that hVPLA2 is associated with cholesterol-sensitive DRMs in both HEK293 and CHO cells.

Copatching of GM1 rafts by cross-linking of hVPLA2. Antibodies or multivalent toxins against membrane components cause lateral cross-linking of the components on the cell membrane by which recruitment of lipid rafts associated with the patched components can be induced around the crossed-linked patch. Thus, antibody-induced copatching of proteins provided a common tool for analyzing lipid rafts association with proteins (17-20). To address the association of hVPLA2 with lipid rafts, CHO cells were treated with hVPLA2 at 12˚C to minimize the metabolic activities of cells and

patching was induced by anti-hVPLA2 and secondary antibody in living cells. Ganglioside GM1 was visualized by staining with CT conjugated with Alexa488. Confocal image analysis revealed that ganglioside GM1-containing rafts were copatched well with the patches of cross-linked hVPLA2, and thus most of the GM1 rafts were colocalized with the patched hVPLA2 (Fig. 3A-C). In the non-patched control cells, GM1 immunostaining showed an even distribution on the cell surface but not on the punctate pattern (Fig. 3D-F). After inducing copatching by cross-linking of hVPLA2, spots of GM1-containing patches (~200-400 nm) were larger than those of the punctate spot of the non-patched control (Fig. 3C and F). By contrast, in the patched cells pretreated with MβCD, the hVPLA2-patch was clearly segregated from the GM1 rafts (Fig. 3I). Depletion of cholesterol by MβCD disrupted the punctate immunostaining of GM1 and hVPLA2 in the non-patched control cells (Fig. 3J and K).

Heparin binding site of hVPLA2 is involved in the association with lipid rafts. Findings of previous studies have demonstrated that hVPLA2 binds to HSPG (13,21) which mediates the association of HSPG-binding proteins such as prion and eosinophil cationic protein with lipid rafts (22,23). To determine whether heparan sulfate binding is involved in the association of hVPLA2 with lipid rafts, we examined whether hVPLA2-W79A/R100E/K101E, a mutant hVPLA2 with deficiency in heparan sulfate binding (Dhs-hVPLA2) was capable of associating with lipid rafts. HEK293 cells were treated with hVPLA2 or Dhs-hVPLA2, subjected to solubilization in Brij-58 and floated onto OptiPrep gradient. Approximately half of Dhs-hVPLA2 in lipid raft fractions was shifted into non-raft fractions (Fig. 4A), while some hVPLA2 remained in lipid raft fractions (Fig. 4B), suggesting that the association of hVPLA2 with lipid rafts was mediated partially through the heparin binding of hVPLA2. In line with this interpretation, confocal image analysis revelaed that cross-linking of Dhs-hVPLA2 was able to recruit GM1 rafts to the mutant hVPLA2 patches, although the mutant hVPLA2 yielded a weaker GM1 immunostaining compared with that of hVPLA2 (Fig. 3C). To clarify whether HSPG is associated with lipid rafts, we performed a copatching experiment in CHO cells with antibody against syndecan, a major subfamily of HSPG. Immunofluorescence staining indicated that syndecan-4 patches were extensively copatched with GM1 rafts, while sydecan-1 patches were clearly separated with GM1 rafts (Fig. 5). These data suggested that since syndecan-4 was associated with lipid rafts in CHO cells, it may be involved in the association of hVPLA2 with lipid rafts.

Flotillin-dependent endocytosis of hVPLA2 in CHO and HEK293 cells. To determine how hVPLA2 is internalized, HEK293 or CHO cells were pretreated with endocytic inhibitors and internalization of hVPLA2 was detected by western blotting. Cell viability was examined subsequent to chemical treatment. As HEK293 cells exhibited sensitivity to the inhibitors, we optimized the conditions to maintain cell viability >90%. Internalization of hVPLA2 was suppressed partially by MβCD and marginally by filipin, a cholesterol sequestration reagent (Fig. 6). However, chlorpromazine, an inhibitor for the endocytosis mediated by clathrin-coated pit
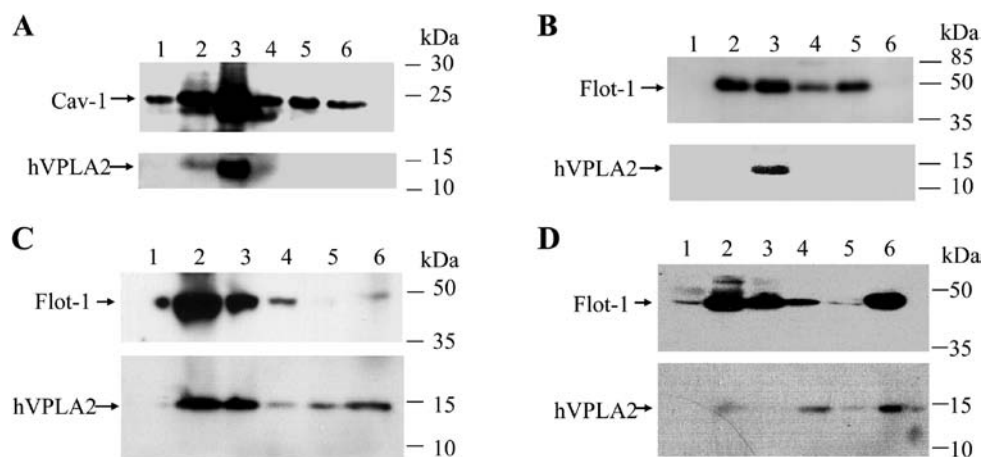
Figure 2. Human group V secretory phospholipase A$_2$ (hVPLA2) is associated with detergent insoluble lipid microdomains in CHO and HEK293 cells. (A) CHO or (B) HEK293 cells were lysed and solubilized in the buffer containing 0.5% Triton X-100. Detergent-resistant membranes (DRMs) from the solubilized lysates were purified using OptiPrep flotation gradients. Fractions from top (lane 1) to bottom (lane 6) were collected following centrifugation. Equal volume from each fraction was precipitated by TCA, resolved by SDS-PAGE and analyzed by western blotting to detect flotillin-1, and hVPLA2 with anti-flottilin-1 and anti-hVPLA2, respectively. To examine the effect of cholesterol depletion on the association of hVPLA2 with lipid rafts, HEK293 cells were incubated (C) without or (D) with 5 mM methy-β-cyclodextrin diluted with DMEM for 2 h at 37°C. DRMs were isolated after solubilization with buffer containing 1% Brij-58. Caveloin-1 was analyzed by western blotting using anti-caveolin-1. Molecular weights on the blots were estimated by a prestained molecular marker (Gibco) or rainbow prestained marker (Amersham). The same electropherogram was obtained from triplicate experiments.
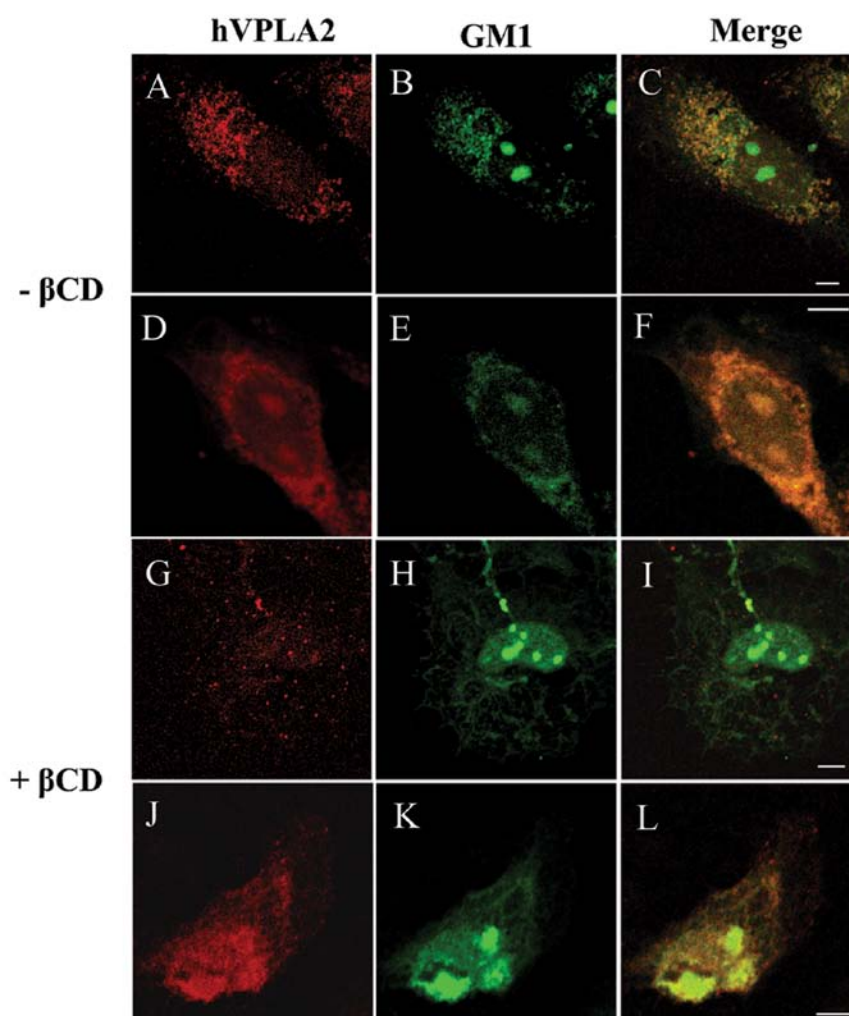

Figure 3. Copatching of ganglioside GM1 by anti-human group V secretory phospholipase A$_2$ (hVPLA2) in CHO. CHO cells were incubated in the (A-F) absence or (G-L) presence of methy-β-cyclodextrin (7.5 mM) for 2 h and treated with hVPLA2 (200 nM). After cross-linking of hVPLA2 by specific mouse anti-hVPLA2 and Alexa568-anti-mouse IgG, the cells were fixed. (D-F and J-L) For the non-patched control, the cells were fixed after incubation with HBSS containing 2% BSA in the absence of specific antibody. Ganglioside GM1 was visualized by Alexa488-cholera toxin B (CT). The left and middle column shows immunofluorescence of hVPLA2 and ganglioside GM1, respectively, and the right column is merged images of the two. Scale bar, 5 μm.
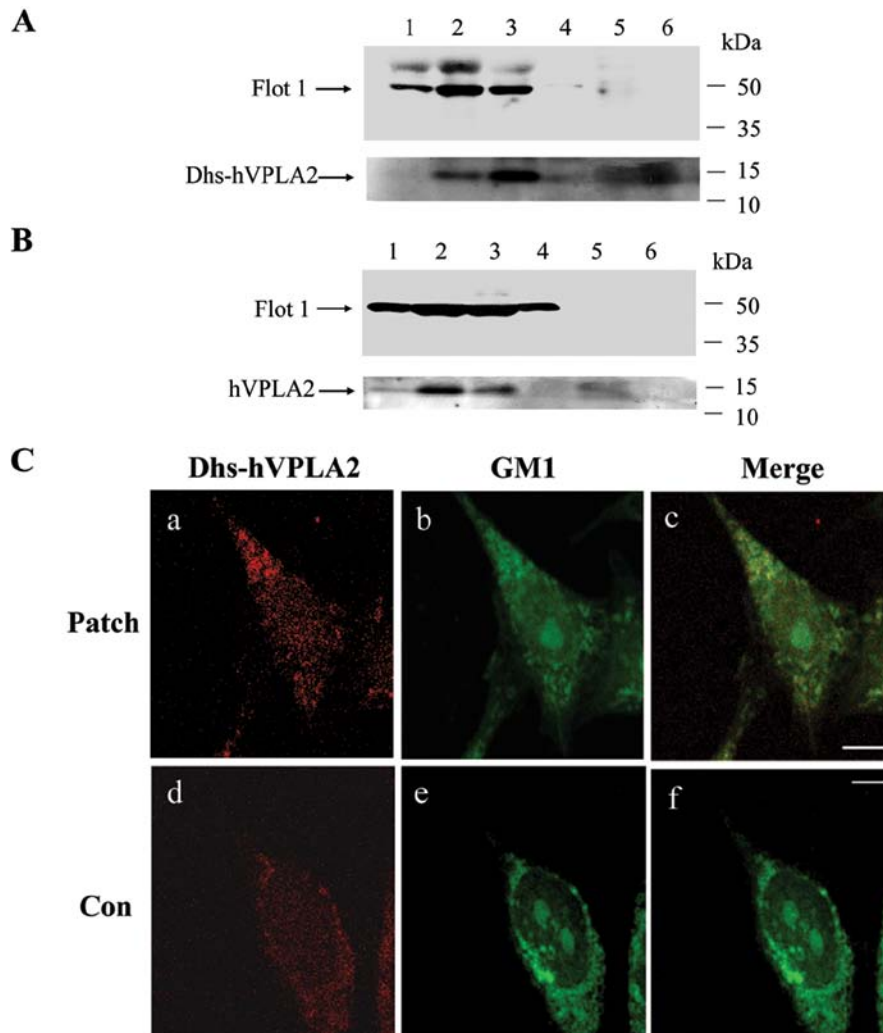
Figure 4. Association of human group V secretory phospholipase A_2 (hVPLA2) with lipid rafts is mediated by heparan sulfate binding. (A and B) HEK293 cells were treated with hVPLA2 or Dhs-hVPLA2, a heparan sulfate-binding mutant, and solubilized in the buffer containing 1% Brij-58 after lysis. Detergent-resistant membranes (DRMs) were isolated by flotation on OptiPrep gradients. Equal amounts of protein from each fraction were resolved by SDS-PAGE and analyzed by western blotting to detect flotillin-1 and hVPLA2 with anti-flotillin-1 and anti-hVPLA2, respectively. (C-a-c) Copatching of ganglioside GM1 by cross-linking of Dhs-hVPLA2 was examined in CHO cells. (d-f) Non-patched control was fixed prior to incubation of the cells with specific antibody against hVPLA2. The left and middle columns show immunofluorescence of hVPLA2 and ganglioside GM1, respectively, and the right column is the merged images of the two. Bar, 5 μm.

had no effect on the internalization of hVPLA2. Pretreatment with N-ethylmaleimide (NEM) and brefeldin A, an inhibitor for the N-ethylmaleimide-sensitive factor (NSF) and a Golgi and endosome traffic disrupting drug, respectively, inhibited endocytosis. Along with the association of hVPLA2 with lipid rafts, these data suggested that hVPLA2 is likely internalized in lipid raft-dependent but not clathrin-dependent pathways. To examine whether lipid rafts were involved in the endocytosis of hVPLA2, we detected hVPLA2 in endocytic vesicles by double immunostaining with flotillin or caveolin. HEK293 or CHO cells were fixed immediately after the endocytosis of hVPLA2 was allowed to occur. To detect the low amount of internalized hVPLA2, we used a relatively high concentration (2 μg/ml) of anti-hVPLA2 and secondary antibody (1/300 dilution), which resulted in non-specific immunostaining inside the nucleus but not cytoplasmic staining (unpublished data). Confocal analysis of double immunostaining revealed extensive colocalization of hVPLA2 with flotillin-1 in the cytoplasmic and perinuclear region in both HEK293 and CHO cells (Fig. 8A-C and G-I). However, hVPLA2 immunostaining was clearly separated from that of caveolin-1 with partial colocalization only in the perinuclear region (Fig. 8D-E and J-L). These data suggest that hVPLA2 associated with lipid rafts on the outside membrane is internalized in vesicles containing flotillin-1 but not caveolin-1. Observation of punctate immunostaining showing that sizes of hVPLA2-positive spots were slightly smaller than those of caveolin-1-positive ones (Fig. 6D-a, g, e and k), suggested that hVPLA2 is likely internalized in vesicles that are different from that resembling a caveolae (50-100 nm). To obtain direct evidence that flotillin-1 mediated the internalization of hVPLA2, we determined the effect of flotillin-1 knockdown on hVPLA2 endocytosis by transfection of siRNA-specific flotillin-1 in HEK293 cells. Knockdown of flotillin-1 markedly inhibited hVPLA2 endocytosis (Fig. 6C). Internalization efficiency of hVPLA2 was 36% in flotillin-1 knockdown cells,
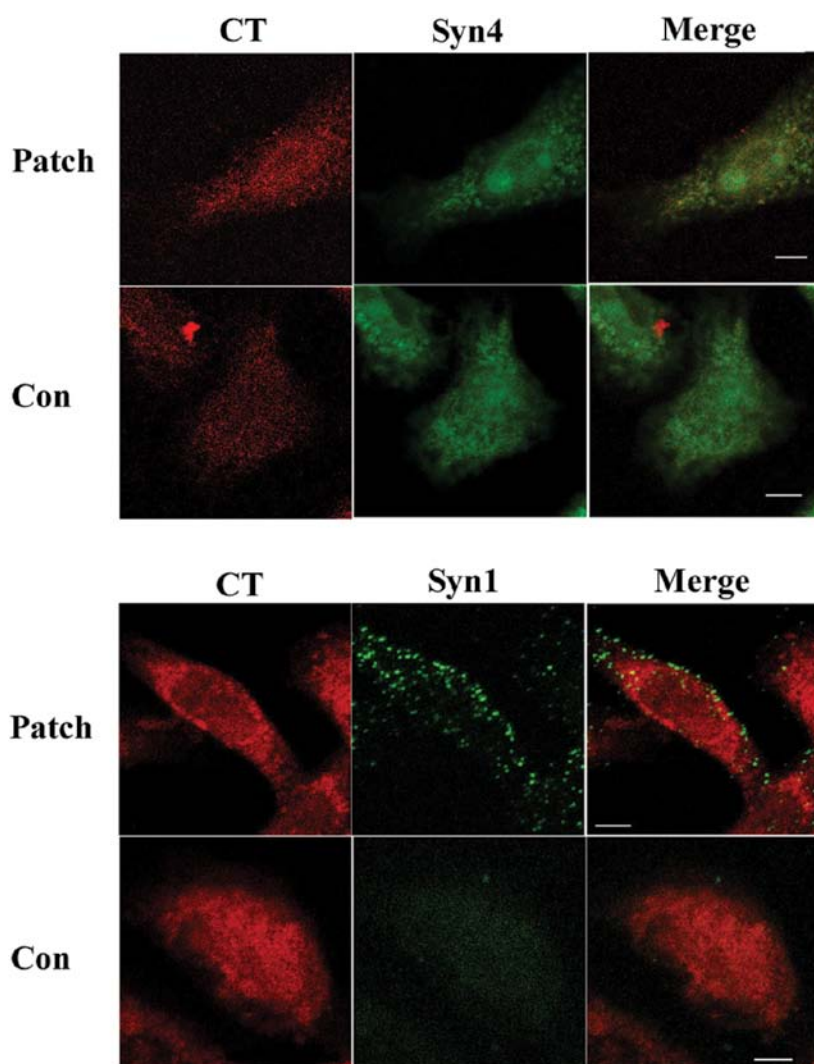
Figure 5. Copatching of ganglioside GM1 by anti-syndecan-4 in CHO cells. The left and middle columns show immunofluorescence of cholera toxin B (CT) and syndecan, respectively, and the right column is the merged images of the two. Cells were incubated with anti-syndecan-4 (Syn4) or anti-syndecan-4 (Syn1). After further cross-linking of syndecan by Alexa488-conjugated secondary antibody, the cells were fixed. For the non-patched control, cells were fixed before incubation of the cells with specific antibody against syndecan-4 or syndecan-1. Ganglioside GM1 was visualized by staining with Alexa568-CT. Bar, 5 μm.

which was normalized against the amount of internalization in the control cells transfected with scrambled siRNA. Considering transfection was regarded as efficient at 90%, the inhibition of hVPLA2 endocytosis by flotillin-1 knockdown was ~72%.

Localization of internalized hVPLA2 into late endocytic compartments and Golgi in HEK293 and CHO cells. To determine the destiny of internalized hVPLA2, the cells were fixed at specific times after treatment with hVPLA2, immunostained and analyzed by confocal microscopy. For the double immunostaining of hVPLA2 and GM130, a low concentration of anti-hVPLA2 (1 μg/ml) and secondary antibody (1/1,000 dilution) were used to minimize non-specific staining. Following a 10-min incubation, internalized hVPLA2 moved partially to the late endocytic compartment containing Lamp-2 as shown by colocalization with Lamp-2 in addition to perinuclear localization (Fig. 7I-N). After 40 min, the colocalization of hVPLA2 around GM130, a cis-Golgi marker was observed. Then, after 90 min, the internalized hVPLA2 was accumu-

lated in large vesicular form around Golgi apparatus as shown in the DIC image (Fig. 7D and H), suggesting that some of the internalized hVPLA2 was not destined to degradation via lysosome but was instead recycled via Golgi.

Effect of lipid rafts on the action mode of hVPLA2 in HEK293 cells. To examine the importance of lipid rafts association in hVPLA2 action on target cells, we examined the effect of disruption of hVPLA2-containing lipid rafts on AA release from the plasma membrane. Our previous result (14) shows that exogenous hVPLA2 treatment generated AA release inside cells for ~5 min in the HEK293 cells. Initial AA release before any significant generation of AA release from inside the membrane can represent AA release from the hVPLA2 action on the plasma membrane. Therefore, steady-state level of AA release was measured at 1 and 5 min with or without MβCD pretreatment. Disruption of association of hVPLA2 with the rafts by MβCD pretreatment enhanced AA release significantly to 1.8- and 2.4-fold 1 and 5 min after hVPLA2 incubation, respectively (Fig. 8). Thus, the association of
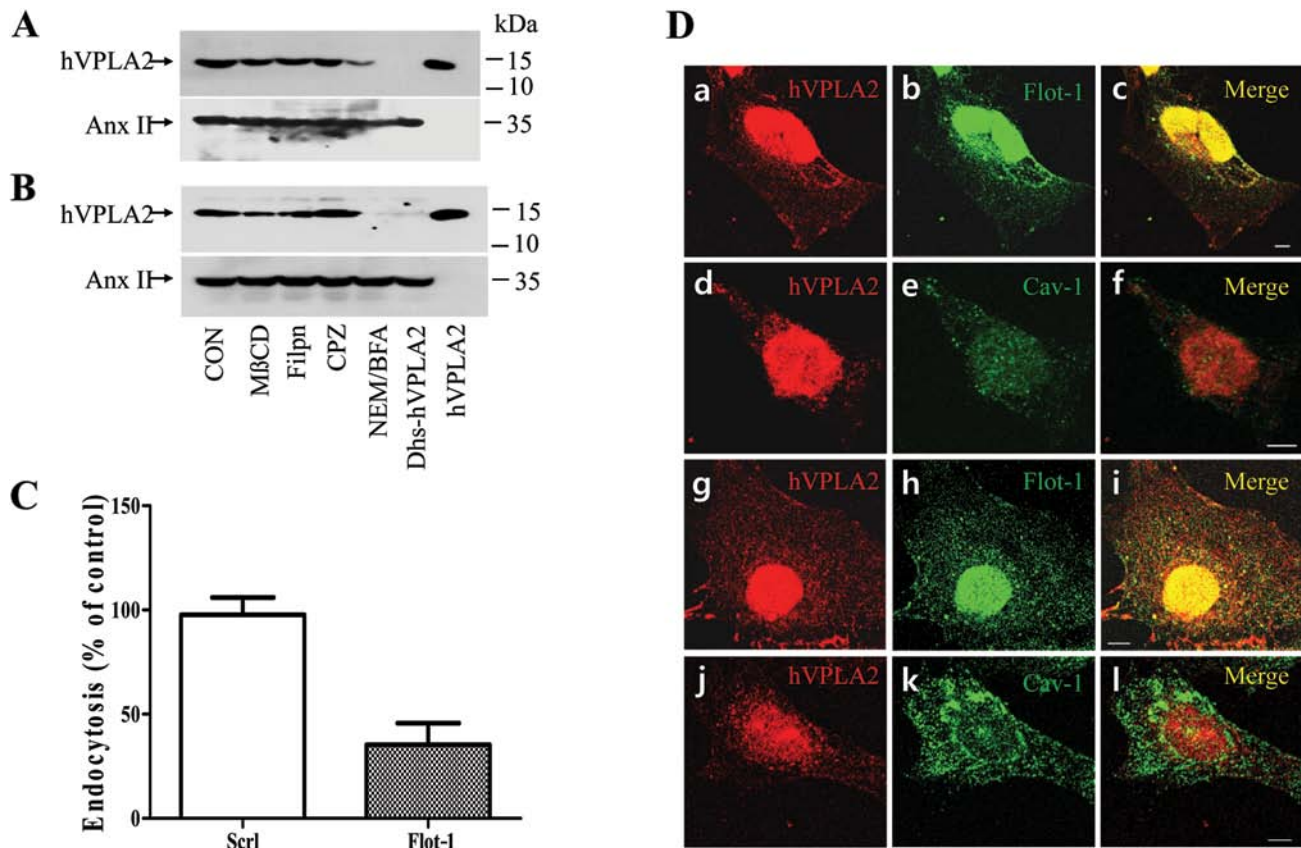
Figure 6. Flotillin-mediated endocytosis of human group V secretory phospholipase A$_2$ (hVPLA2) in HEK 293 and CHO cells. (A and B) Effect of inhibitors on the internalization of hVPLA2 was examined in (A) HEK293 or (B) CHO cells. The cells were incubated in the presence of 7.5 mM methy-β-cyclodextrin (MβCD), 1 μg/ml of filipin III (Filpn), or 10 μg/ml of chlorpromazine (CPZ) for 90 min. N-ethylmaleimide (NEM; 100 mM) and 10 μg/ml of brefeldin A (BFA) was treated for 45 min at 37°C. The cells were treated with 100 nM hVPLA2 or Dhs-hVPLA2 for 20 min at 37°C. After washing with DMEM or Ham containing 0.8 M NaCl, the cells were lysed. Equal amounts of protein were subjected to 16% SDS-PAGE and analyzed by western blotting. As reference controls, blots were stripped and reprobed with rabbit anti-annexin II. As a positive control for SDS-PAGE and western blotting, authentic hVPLA2 was used. Molecular weights on the blots were estimated by rainbow prestained marker. The electropherogram was representative of three independent experiments. (C) Effect of flotillin-1 knockdown on endocytosis of hVPLA2 was examined in HEK293 cells by tranfection with siRNA for flotillin-1 (Flot-1) or scrambled (Scrl) control siRNA. After applying 150 nM of hVPLA2 to the transfected cells for 30 min, the extent of endocytosis was determined by the enzymatic activities of internalized hVPLA2 as described in Materials and methods. The data presents the mean ± SE from two independent experiments performed in triplicate. (D) Colocalization of internalized hVPLA2 with Flot-1 or caveolin-1 (Cav-1) was determined in (a-f) HEK 293and (g-l) CHO cells After treating HEK293 and CHO cells with 100 nM hVLA2, cells were double immunostained (a-c and g-i) for hVPLA2 and Flot-1 or (d-f and j-l) for hVPLA2 and Cav-1. The left and middle columns show immunostaining of hVPLA2 and Flot-1 (or Cav-1), respectively. Bar, 5 μm.

hVPLA2 with lipid rafts resulted in a reduction of AA release from the plasma membrane.

Discussion

Despite extensive studies on sPLA2, its mode of action and internalization mechanisms remain largely unknown. In the present study, we have shown that hVPLA2 is associated with lipid rafts and internalized in a flotillin-dependent pathway. The association of hVPLA2 with lipid rafts was shown by cholesterol-sensitive enrichment of hVPLA2 in low-density DRM fraction and copatching of GM1 rafts through hVPLA2 cross-linking in a cholesterol-sensitive manner (Figs. 2 and 3). As Dhs-hVPLA2, a mutant hVPLA2 deficient in binding to heparan sulfate, distributed dispersedly in both low-density and high-density fraction, binding to HSPG may be necessary for the association of hVPLA2 with lipid rafts (Figs. 4 and 5). In addition, cross-linking of Dhs-hVPLA2 may recruit GM1 rafts less efficiently than that of hVPLA2, even though residual copatching of GM1 was induced (Figs. 3C and 4C).

We then determined whether HSPG is associated with lipid rafts to mediate recruiting hVPLA2 to lipid rafts. Copatching experiment with antibody against syndecan, a major family of HSPG showed that lipid rafts containing syndecan-4 but not syndecan-1 recruited with GM1 rafts efficiently. Immunostaining in unpatched control cells showed a punctate pattern of syndecan-1 (Fig. 5), indicating that syndecan-1 may be associated with lipid rafts, although syndecan-1 did not recruit GM1 rafts. This interpretation is supported by a recent finding that syndecan-1 and -4 are specifically associated with sphingomyelin-enriched lipid rafts in parathyroid cell (24). Taken together, these data suggested that additional interaction other than heparan sulfates with molecules residing in lipid rafts may be necessary for association of hVPLA2 with lipid rafts.

Internalization of hVPLA2 was shown to occur in a flotillin-dependent mechanism by flotillin-1 knockdown and endocytic inhibitors. Internalization of hVPLA2 was determined based on the enzyme activity of hVPLA2 and immunocytochemistry using a specific antibody against
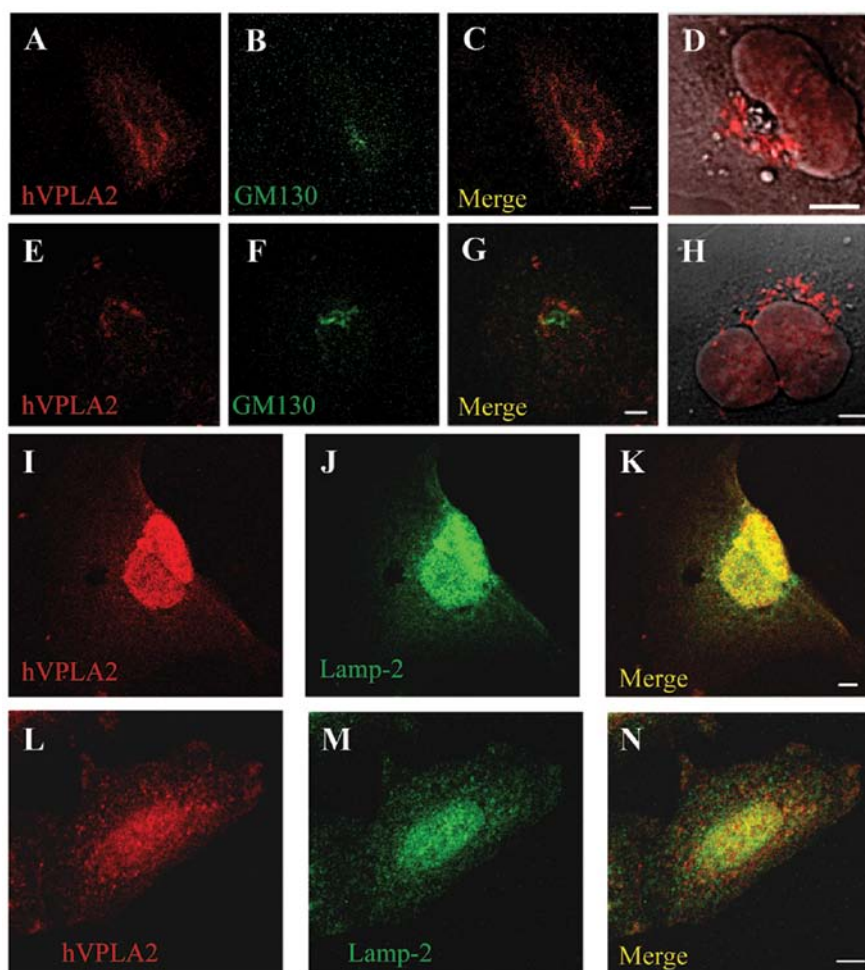
Figure 7. Intracellular localization of internalized human group V secretory phospholipase A$_2$ (hVPLA2) in lysozyme and Golgi apparatus. (A-D and I-K) HEK293 and (E-H and L-N) CHO cells were treated with hVPLA2, fixed at specific times, and immunostained with antibody against (A-C and E-G) hVPLA2 and GM130 (cis-Golgi marker) 40 min after hVPLA2 treatment or (I-K and M-O) hVPLA2 and Lamp-2 10 min after treatment. DIC image of internalized hVPLA2 in (D) HEK293 and (H) CHO cells 90 min after treatment showed that internalized hVPLA2 was localized diffusely around Golgi apparatus. Bar, 5 μm.
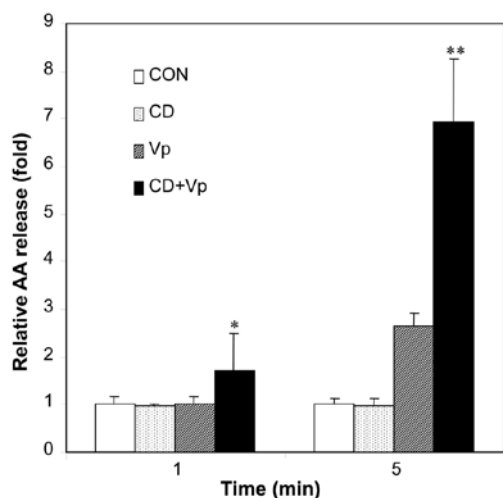

Figure 8. Effect of methy-β-cyclodextrin (MβCD) on the human group V secretory phospholipase A$_2$ (hVPLA2)-induced arachidonic acid (AA) release in CHO cells. CHO cells were cultivated in the presence or absence of 5 mM MβCD for 90 min and treated with hVPLA2 or medium only for a given time. Culture supernatants were collected immediately after quenching the reaction. Relative AA release to the control samples was calculated by measuring radioactivity in the supernatants and cell pellets. The data present the mean of triplicate samples from two independent experiments in which the value from cells treated with hVPLA2 (Vp) in the absence versus in the presence of MβCD (CD) is significantly different (n=6, *P<0.05, **P<0.01).

hVPLA2. Internalization kinetics showed that the half-life of internalization was 16 min and the plateau was attained in 70 min. As some of the internalized hVPLA2 was destined to late endosome or lysosome within which hVPLA2 lost enzymatic activity (Fig. 7), determination of the internalization rate based on enzyme activity would be underestimated and may represent the sum of complex kinetics including internalization, trafficking, and degradation. Rough estimation of internalization rate, and relatively rapid internalization ($t_{1/2}$ =16 min) suggested that the internalization rate is consistent with nonclathrin endocytosis. Consistent with these data, chlorpromazine, an inhibitor of clathrin-mediated endocytosis did not inhibit hVPLA2 internalization, whereas, MβCD, a specific cholesterol-depletion drug, attenuated hVPLA2 internalization. However, filipin, a cholesterol-sequestrating drug that suppresses caveolin-mediated endocytosis was slightly inhibited, suggesting that hVPLA2 was internalized in a non-caveolin endocytic route. Results of the flotillin knockdown experiment revealed that flotillin-1 is responsible for hVPLA2 endocytosis. In addition, internalized hVPLA2 was extensively colocalized with flotillin-1 in the punctate structures, although not with caveolin-1. Unlike our result, murine VPLA2 tagged with GFP was shown to be localized

in caveolin-2-containing granules in LPS-stimulated P388D1 macrophage-like cells (13). This difference in the localization of VPLA2 may reflect the difference in cell type. In addition, VPLA2-GFP expressed in secreting granules in P388D1 cells can interfere with imaging of reuptake of secreted VPLA2-GFP. These data have shown that hVPLA2 is internalized in a flotillin-dependent pathway in HEK293 cells. Previous studies have shown that cationic molecules including polyamines, polypeptide and polyplexes enter cells through HSPG and are endocytosed in a flotillin-dependent route in BS-C-1 cells (25,26), which is consistent with our result. However, contrary to our result showing that hVPLA2 was trafficked not only to the lysosomal compartments, but also to Golgi, the internalized cationic molecules bound to HSPG were trafficked predominantly to late endosome within 120 min, but not to Golgi apparatus. Different cell type or additional interaction of hVPLA2 with lipid rafts other than the interaction through heparan sulfate, which may control interaction with trafficking adaptors, may contribute to this difference in trafficking routes. The trafficking of internalized hVPLA2 to non-lysosomal vesicles and later to Golgi (Fig. 7) shows that some of the hVPLA2 is delivered to other targets instead of degradation. Consistent with this result, it is reported that AA is generated from inside the membrane following treatment with exogenous hVPLA2 (10,14).

To get insight on the role of lipid rafts in the regulation of hVPLA2 action, we determined AA release from the plasma membrane in the presence or absence of MβCD. Disruption of the association with lipid rafts hVPLA2 by MβCD pretreatment increased AA release from the plasma membrane up to 2.45-fold compared with absence of MβCD pretreatment. These data can be interpreted in different ways. One is that limited diffusion and clustering of hVPLA2 in lipids rafts enriched in cholesterol and glycosphingolipids have limited access to PC, a major substrate outside the plasma membrane. Another reason involves reduced residence time in the plasma membrane by relatively rapid internalization of hVPLA2 associated with lipid rafts to intracellular targets. When CHO cells were treated with MβCD to disrupt lipid rafts and treated with hVPLA2 (150 nM), extensive conversion of PC (>15%) into the lysoPC in plasma membrane occurred, resulting in cell death (unpublished data). The localization of some of the internalized hVPLA2 in Lamp 2-negative punctate structures and later around the Golgi complex indicated that internalized hVPLA2 is capable of inducing AA release from the intracellular target sites instead of degradation inside the lysosomal compartments. Therefore, these data suggest that the association of hVPLA2 with lipid rafts may play a role in protecting plasma membrane from excessive degradation and increasing AA release and eicosanoid production coupled with released AA from intracellular targets.

Acknowledgements

References

1. Schaloske RH and Dennis EA: The phospholipase A_2 superfamily and its group numbering system. Biochim Biophys Acta 1761: 1246-1259, 2006.
2. Lambeau G and Gelb MH: Biochemistry and physiology of mammalian secreted phospholipases A_2. Annu Rev Biochem 77: 495-520, 2008.
3. Han WK, Sapirstein A, Hung CC, Alessandrini A and Bonventre JV: Cross-talk between cytosolic phospholipase A_2 alpha (cPLA$_2$ alpha) and secretory phospholipase A_2 (sPLA$_2$) in hydrogen peroxide-induced arachidonic acid release in murine mesangial cells: sPLA$_2$ regulates cPLA$_2$ alpha activity that is responsible for arachidonic acid release. J Biol Chem 278: 24153-24163, 2003.
4. Murakami M, Kambe T, Shimbara S, Yamamoto S, Kuwata H and Kudo I: Functional association of type IIA secretory phospholipase A(2) with the glycosylphosphatidylinositol-anchored heparan sulfate proteoglycan in the cyclooxygenase-2-mediated delayed prostanoid-biosynthetic pathway. J Biol Chem 274: 29927-29936, 1999.
5. Fleisch JH, Armstrong CT, Roman CR, *et al*: Recombinant human secretory phospholipase A2 released thromboxane from guinea pig bronchoalveolar lavage cells: in vitro and ex vivo evaluation of a novel secretory phospholipase A2 inhibitor. J Pharmacol Exp Ther 278: 252-257, 1996.
6. Kim YJ, Kim KP, Han SK, *et al*: Group V phospholipase A_2 induces leukotriene biosynthesis in human neutrophils through the activation of group IVA phospholipase A_2. J Biol Chem 277: 36479-36488, 2002.
7. Muñoz NM, Kim YJ, Meliton AY, *et al*: Human group V phospholipase A_2 induces group IVA phospholipase A_2-independent cysteinyl leukotriene synthesis in human eosinophils. J Biol Chem 278: 38813-38820, 2003.
8. Bezzine S, Koduri RS, Valentin E, *et al*: Exogenously added human group X secreted phospholipase A(2) but not the group IB, IIA, and V enzymes efficiently release arachidonic acid from adherent mammalian cells. J Biol Chem 275: 3179-3191, 2000.
9. Murakami M, Koduri RS, Enomoto A, *et al*: Distinct arachidonate-releasing functions of mammalian secreted phospholipase A2s in human embryonic kidney 293 and rat mastocytoma RBL-2H3 cells through heparan sulfate shuttling and external plasma membrane mechanisms. J Biol Chem 276: 10083-10096, 2001.
10. Wijewickrama GT, Kim JH, Kim YJ, *et al*: Systematic evaluation of transcellular activities of secretory phospholipases A_2. High activity of group V phospholipases A_2 to induce eicosanoid biosynthesis in neighboring inflammatory cells. J Biol Chem 281: 10935-10944, 2006.
11. Reddy ST and Herschman HR: Transcellular prostaglandin production following mast cell activation is mediated by proximal secretory phospholipase A_2 and distal prostaglandin synthase 1. J Biol Chem 271: 186-191, 1996.
12. Murakami M, Kambe T, Shimbara S and Kudo I: Functional coupling between various phospholipase A_2s and cyclooxygenases in immediate and delayed prostanoid biosynthetic pathways. J Biol Chem 274: 3103-3115, 1999.
13. Balboa MA, Shirai Y, Gaietta G, Ellisman MH, Balsinde J and Dennis EA: Localization of group V phospholipase A_2 in caveolin-enriched granules in activated P388D$_1$ macrophage-like cells. J Biol Chem 278: 48059-48065, 2003.
14. Kim YJ, Kim KP, Rhee HJ, *et al*: Internalized group V secretory phospholipase A_2 acts on the perinuclear membranes. J Biol Chem 277: 9358-9365, 2002.
15. Han SK, Kim KP, Koduri R, *et al*: Roles of Trp31 in high membrane binding and proinflammatory activity of human group V phospholipase A_2. J Biol Chem 274: 11881-11888, 1999.
16. Glebov OO, Bright NA and Nichols BJ: Flotillin-1 defines a clathrin-independent endocytic pathway in mammalian cells. Nat Cell Biol 8: 46-54, 2006.
17. Harder T, Scheiffele P, Verkade P and Simons K: Lipid domain structure of the plasma membrane revealed by patching of membrane components. J Cell Biol 141: 929-942, 1998.
18. Janes PW, Ley SC and Magee AI: Aggregation of lipid rafts accompanies signaling via the T cell antigen receptor. J Cell Biol 147: 447-461, 1999.
19. Ringerike T, Blystad FD, Levy FO, Madshus IH and Stang E: Cholesterol is important in control of EGF receptor kinase activity but EGF receptors are not concentrated in caveolae. J Cell Sci 115: 1331-1340, 2002.

20. Roepstorff K, Thomsen P, Sandvig K and van Deurs B: Sequestration of epidermal growth factor receptors in non-caveolar lipid rafts inhibits ligand binding. J Biol Chem 277: 18954-18960, 2002.

21. Kim KP, Rafter JD, Bittova L, et al: Mechanism of human group V phospholipase A_2 (PLA_2)-induced leukotriene biosynthesis in human neutrophils. A potential role of heparan sulfate binding in PLA_2 internalization and degradation. J Biol Chem 276: 11126-11134, 2001.

22. Fan TC, Chang HT, Chen IW, Wang HY and Chang MD: A heparan sulfate-facilitated and raft-dependent macropinocytosis of eosinophil cationic protein. Traffic 8: 1778-1795, 2007.

23. Taylor DR, Whitehouse IJ and Hooper NM: Glypican-1 mediates both prion protein lipid raft association and disease isoform formation. PLoS Pathog 5: e1000666, 2009.

24. Podyma-Inoue KA, Hara-Yokoyama M, Shinomura T, Kimura T and Yanagishita M: Syndecans reside in sphingomyelin-enriched low-density fractions of the plasma membrane isolated from a parathyroid cell line. PloS One 7: e32351, 2012.

25. Payne CK, Jones SA, Chen C and Zhuang X: Internalization and trafficking of cell surface proteoglycans and proteoglycan-binding ligands. Traffic 8: 389-401, 2007.

26. Vercauteren D, Piest M, van der Aa LJ, et al: Flotillin-dependent endocytosis and a phagocytosis-like mechanism for cellular internalization of disulfide-based poly(amido amine)/DNA polyplexes. Biomaterials 32: 3072-3084, 2011.